

**Reactivity of  $[\text{Mn}_2(\mu\text{-H})_2(\text{CO})_6(\mu\text{-tedip})]$  (tedip =  $(\text{EtO})_2\text{POP}(\text{OEt})_2$ ) with Group 11 Alkynyl Compounds. X-ray Structures of  $[\text{Ag}_2\text{Mn}_4(\mu\text{-H})_6(\text{CO})_{12}(\mu\text{-tedip})_2]$  and  $[\text{AuMn}_4(\mu\text{-H})_5(\text{CO})_{12}(\mu\text{-tedip})_2]$**

Remedios Carreño, Víctor Riera,\* and Miguel A. Ruiz

*Departamento de Química Organometálica, Universidad de Oviedo, E-33071 Oviedo, Spain*

Antonio Tiripicchio and Marisa Tiripicchio-Camellini

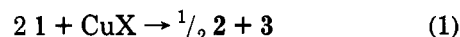
*Istituto di Chimica Generale ed Inorganica, Centro di Studio per la Strutturistica Diffattometrica del CNR, Università di Parma, Viale delle Scienze 78, I-43100, Parma, Italy*

Received August 3, 1993\*

The unsaturated dihydride  $[\text{Mn}_2(\mu\text{-H})_2(\text{CO})_6(\mu\text{-tedip})]$  (1; tedip =  $(\text{EtO})_2\text{POP}(\text{OEt})_2$ ) reacts at room temperature with  $[\text{M}(\text{C}\equiv\text{CPh})]_n$  ( $\text{M} = \text{Cu}, \text{Ag}$ ) to give a mixture of the hydrido alkynyl complex  $[\text{Mn}_2(\mu\text{-H})(\mu\text{-}\eta^1\text{:}\eta^2\text{-}(\text{C}\equiv\text{CPh})(\text{CO})_6(\mu\text{-tedip}))]$  (4) and the corresponding hexanuclear clusters  $[\text{M}_2\text{Mn}_4(\mu\text{-H})_6(\text{CO})_{12}(\mu\text{-tedip})_2]$  ( $\text{M} = \text{Cu}$  (2),  $\text{Ag}$  (5)), all displaying fluxional behavior in solution. In contrast, reaction of 1 with  $[\text{Au}(\text{C}\equiv\text{CPh})]_n$  yields the pentanuclear cluster  $[\text{AuMn}_4(\mu\text{-H})_5(\text{CO})_{12}(\mu\text{-tedip})_2]$  (6), also fluxional, along with complex 4. The structures of clusters 5 and 6 have been determined by X-ray diffraction methods. Crystals of 5 are triclinic, space group  $P\bar{1}$ , with  $Z = 1$  in a unit cell of dimensions  $a = 14.014(9)$  Å,  $b = 9.272(7)$  Å,  $c = 10.741(6)$  Å,  $\alpha = 102.91(2)^\circ$ ,  $\beta = 107.01(2)^\circ$ , and  $\gamma = 103.37(2)^\circ$ . The structure has been solved from diffractometer data by Patterson and Fourier methods and refined by full-matrix least squares on the basis of 3027 observed reflections to  $R$  and  $R_w$  values of 0.0547 and 0.0622, respectively. Complex 5 is centrosymmetric and exhibits a planar  $\text{Ag}_2\text{Mn}_4$  core consisting of a  $\text{Ag}_2\text{Mn}_2$  lozenge with two further Mn atom "spikes" in the plane of the Ag atoms. The Ag–Ag bond distance is 2.800(2) Å, whereas the three Ag–Mn bond distances are rather different, 2.751(2), 2.902(2), and 3.050(2) Å; the Mn–Mn separations of 3.312(3) Å are rather long and are probably indicative of a very small direct bonding interaction between manganese atoms. Even though an accurate location of the hydrides was not possible, there is substantial evidence that four of them bridge Ag–Mn edges and two triply bridge the  $\text{Mn}_2\text{Ag}$  faces. Crystals of 6 are triclinic, space group  $P\bar{1}$ , with  $Z = 2$  in a unit cell of dimensions  $a = 18.356(7)$  Å,  $b = 11.952(5)$  Å,  $c = 11.688(5)$  Å,  $\alpha = 74.37(2)^\circ$ ,  $\beta = 78.86(2)^\circ$ , and  $\gamma = 83.42(2)^\circ$ . The structure has been solved from diffractometer data by Patterson and Fourier methods and refined by full-matrix least squares on the basis of 5266 observed reflections to  $R$  and  $R_w$  values of 0.0433 and 0.0471, respectively. The metal core of complex 6 consists of two  $\text{AuMn}_2$  triangles sharing the common Au vertex and tilted by  $21.1(1)^\circ$ . The two Mn–Mn separations are different, 2.860(2) and 3.080(2) Å. There is strong evidence that three hydrides bridge the edges of the triangle with the longer Mn–Mn distance, whereas the other triangle supports a triply bridging hydride and an edge-bridging (Mn–Mn) hydride. In contrast with the previous reactions,  $[\text{Mn}_2(\mu\text{-H})_2(\text{CO})_6(\mu\text{-tedip})]$  and  $[\text{Au}(\text{C}\equiv\text{CR})(\text{PR}'_3)]$  ( $\text{R} = \text{Ph}$ ,  $\text{R}' = p\text{-tol}$ ;  $\text{R} = \text{tBu}$ ,  $\text{R}' = \text{Ph}$ ) give the trimetallic clusters  $[\text{Mn}_2\mu\text{-Au}(\text{PR}'_3)(\mu\text{-}\eta^1\text{:}\eta^2\text{-CH=CHR})(\text{CO})_6(\mu\text{-tedip})]$  in good yields, having *trans*-alkenyl ligands, as indicated by NMR data.

### Introduction

Recently, we reported the synthesis of several manganese–group 11 metal and manganese–zinc clusters derived from the unsaturated dihydride  $[\text{Mn}_2(\mu\text{-H})_2(\text{CO})_6(\mu\text{-tedip})]$  ( $\text{Mn} = \text{Mn}$ ) (1; tedip =  $(\text{EtO})_2\text{POP}(\text{OEt})_2$ ).<sup>1</sup> In that paper we described the reaction between 1 and copper(I) halides ( $\text{CuX}$ ;  $\text{X} = \text{Cl}, \text{Br}, \text{I}$ ) which unexpectedly yielded the planar "raft" hexametallate cluster  $[\text{Cu}_2\text{Mn}_4(\mu\text{-H})_6(\text{CO})_{12}(\mu\text{-tedip})_2]$ <sup>1,2</sup> (2) and the corresponding halogeno complexes  $[\text{Mn}_2(\mu\text{-H})(\mu\text{-X})(\text{CO})_6(\mu\text{-tedip})]$  (3) (eq 1). The above method, however, could not be used to synthesize



related silver or gold clusters. Heterometallic group 11 metal clusters in which no phosphine ligands are attached to the coinage metal are scarce.<sup>3</sup> Those exhibiting planar cores and having hydrido ligands are even fewer and are restricted so far to  $\text{Re}_4\text{Cu}_2$ ,<sup>4</sup>  $\text{Rh}_3\text{Ag}_3$ ,<sup>5</sup>  $\text{Os}_3\text{Cu}_3$ ,<sup>6</sup> or  $\text{Nb}_3\text{Au}_3$ <sup>7</sup> metal cores.

(3) Salter, I. D. *Adv. Organomet. Chem.* 1989, 29, 249.

(4) (a) Rhodes, L. F.; Huffman, J. C.; Caulton, K. G. *J. Am. Chem. Soc.* 1983, 105, 5137. (b) Sutherland, B. R.; Ho, D. M.; Huffman, J. C.; Caulton, K. G. *Angew. Chem., Int. Ed. Engl.* 1987, 26, 135.

(5) Bachechi, F.; Ott, J.; Venanzi, L. M. *J. Am. Chem. Soc.* 1985, 107, 1760.

(6) Lemmen, T. H.; Huffman, J. C.; Caulton, K. G. *Angew. Chem., Int. Ed. Engl.* 1986, 25, 262.

(7) Antiñolo, A.; Jalón, F. A.; Otero, A.; Fajardo, M.; Chaudret, B.; Lahoz, F.; López, J. A. *J. Chem. Soc., Dalton Trans.* 1991, 1861.

\* Abstract published in *Advance ACS Abstracts*, February 1, 1994.  
(1) Riera, V.; Ruiz, M. A.; Tiripicchio, A.; Tiripicchio-Camellini, M. *Organometallics* 1993, 12, 2962.

(2) Riera, V.; Ruiz, M. A.; Tiripicchio, A.; Tiripicchio-Camellini, M. *J. Chem. Soc., Chem. Commun.* 1985, 1505.



Table 1. IR and  $^{31}\text{P}$  NMR Data for New Compounds

compd	$\nu(\text{CO})^a/\text{cm}^{-1}$	$^{31}\text{P}\{\text{H}\}$ NMR $^b/\delta$
$[\text{Mn}_2(\mu\text{-H})(\mu\text{-C}\equiv\text{CPh})(\text{CO})_6(\mu\text{-tedip})]$ (4)	2053 s, 2023 s, 1981 s, 1964 s, 1946 vs	164.3 (s)
$[\text{Ag}_2\text{Mn}_4(\mu\text{-H})_6(\text{CO})_{12}(\mu\text{-tedip})_2]$ (5)	2035 vs, 2017 m, 1970 s, 1946 s	171.0 (s)
$[\text{AuMn}_4(\mu\text{-H})_3(\text{CO})_{12}(\mu\text{-tedip})_2]$ (6)	2034 s, 2029 s, 2015 vs, 1973 s, 1954 m, 1942 s, 1933 sh, m, 1927 sh, w	169.2 (s)
$[\text{Mn}_2(\mu\text{-AuP}(\text{p-tol})_3)(\mu\text{-CH}=\text{CHPh})(\text{CO})_6(\mu\text{-tedip})]$ (7)	2030 vw, 2007 vw, 1952 s, 1923 vs, 1887 s, 1852 m <sup>c</sup>	186.3 (d, 65, <sup>d</sup> MnP), 172.9 (d, 65, <sup>b</sup> MnP), 44.9 (s, AuP)
$[\text{Mn}_2(\mu\text{-AuPPh}_3)(\mu\text{-CH}=\text{CH}^t\text{Bu})(\text{CO})_6(\mu\text{-tedip})]$ (8)	2032 vw, 2009 vw, 1949 s, 1916 vs, 1873 s, 1842 s <sup>c</sup>	186.1 (d, 64, <sup>d</sup> MnP), 172.7 (d, 64, <sup>d</sup> MnP), 46.0 (s, AuP)

<sup>a</sup> In petroleum ether solution, unless otherwise stated. <sup>b</sup> At 121.45 MHz, in  $\text{C}_6\text{D}_6$  solution at room temperature. <sup>c</sup> Toluene solution. <sup>d</sup>  $J_{\text{PP}}$  in Hz.

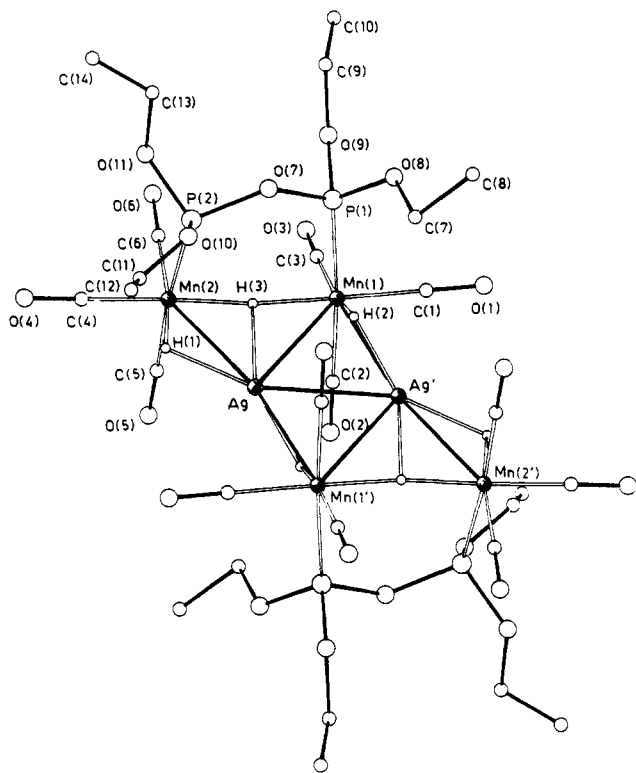


Figure 1. Molecular structure of  $[\text{Ag}_2\text{Mn}_4(\mu\text{-H})_6(\text{CO})_{12}(\mu\text{-tedip})_2]$  (5) with the atom-numbering scheme. The positions of the hydrides could not be established unambiguously.

NMR spectra of 5 remained virtually unchanged down to 183 K, except for the expected changes in line widths. This different dynamic behavior prompted us to examine the crystal structure of compound 5.

The structure of 5 is depicted in Figure 1, together with the atom-numbering scheme. A summary of the important bond distances and angles is given in Table 2. The complex is a centrosymmetric planar dimer (with the crystallographic center of symmetry at the midpoint of the Ag–Ag bond) with the  $\text{Ag}_2\text{Mn}_4$  core, which can be described as a  $\text{Ag}_2\text{Mn}_2$  lozenge with two further Mn atom “spikes” in the plane of the Ag atoms. The  $\text{Ag}_2\text{Mn}_4$  core strongly resembles that previously found in the copper analogue<sup>2</sup> (Figure 2a,b). There is a small but significant distortion of the central lozenge in 5 (overemphasized in Figure 2b) so that the Mn(1)–Ag and Mn(1)–Ag' distances (3.050(2) and 2.902(2) Å) now differ by ca. 0.15 Å, whereas in the copper cluster the difference between the Mn(1)–Cu and Mn(1)–Cu' distances is ca. 0.05 Å. This tends to weaken one of the Mn–Ag bonds, so that one could conceive a fused-square skeleton (shown in Figure 2c) as the extreme result of this distortion, a point of view which will help in the interpretation of the NMR spectra of 5. The Mn(1)–Mn(2) separation (3.312(2) Å) is comparable to that found in 2 (3.282(3) Å) and is out of the usual range

Table 2. Important Interatomic Distances (Å) and Angles (deg) for Compound 5<sup>a</sup>

Ag–Ag'	2.800(2)	P(1)–O(7)	1.625(6)
Ag–Mn(1)	3.050(2)	P(1)–O(8)	1.591(8)
Ag–Mn(2)	2.751(2)	P(1)–O(9)	1.571(7)
Ag'–Mn(1)	2.902(2)	P(2)–O(7)	1.618(7)
Mn(1)–P(1)	2.214(2)	P(2)–O(10)	1.592(12)
Mn(1)–C(1)	1.783(11)	P(2)–O(11)	1.582(8)
Mn(1)–C(2)	1.829(8)	C(1)–O(1)	1.170(14)
Mn(1)–C(3)	1.808(11)	C(2)–O(2)	1.122(10)
Mn(2)–P(2)	2.204(3)	C(3)–O(3)	1.135(14)
Mn(2)–C(4)	1.777(11)	C(4)–O(4)	1.157(14)
Mn(2)–C(5)	1.820(11)	C(5)–O(5)	1.133(14)
Mn(2)–C(6)	1.801(12)	C(6)–O(6)	1.136(17)
Mn(1)–Ag–Mn(2)	69.4(1)	C(4)–Mn(2)–C(6)	93.7(5)
Ag'–Ag–Mn(1)	59.3(1)	C(5)–Mn(2)–C(6)	93.7(6)
Ag'–Ag–Mn(2)	128.6(1)	Mn(1)–P(1)–O(7)	116.8(2)
Ag'–Ag–Mn(1')	64.6(1)	Mn(1)–P(1)–O(8)	120.3(3)
Ag–Mn(1)–Ag'	56.1(1)	Mn(1)–P(1)–O(9)	113.9(3)
Ag–Mn(1)–P(1)	99.6(1)	O(7)–P(1)–O(8)	99.6(3)
Ag–Mn(1)–C(1)	132.6(3)	O(7)–P(1)–O(9)	103.6(4)
Ag–Mn(1)–C(2)	75.7(3)	O(8)–P(1)–O(9)	99.8(4)
Ag–Mn(1)–C(3)	134.0(3)	Mn(2)–P(2)–O(7)	118.3(3)
Ag'–Mn(1)–P(1)	106.1(1)	Mn(2)–P(2)–O(10)	120.8(4)
Ag'–Mn(1)–C(1)	76.5(3)	Mn(2)–P(2)–O(11)	110.6(4)
Ag'–Mn(1)–C(2)	73.6(3)	O(7)–P(2)–O(10)	94.6(5)
Ag'–Mn(1)–C(3)	158.7(3)	O(7)–P(2)–O(11)	103.1(4)
P(1)–Mn(1)–C(1)	93.0(3)	O(10)–P(2)–O(11)	107.1(6)
P(1)–Mn(1)–C(3)	91.3(3)	P(1)–O(7)–P(2)	129.7(4)
C(1)–Mn(1)–C(2)	92.0(4)	P(1)–O(8)–C(7)	122.5(6)
C(1)–Mn(1)–C(3)	90.7(5)	P(1)–O(9)–C(9)	123.5(8)
C(2)–Mn(1)–C(3)	90.3(4)	P(2)–O(10)–C(11)	123.9(18)
Ag–Mn(2)–P(2)	89.0(1)	P(2)–O(11)–C(13)	121.9(11)
Ag–Mn(2)–C(4)	118.2(3)	Mn(1)–C(1)–O(1)	178.0(9)
Ag–Mn(2)–C(5)	85.0(4)	Mn(1)–C(2)–O(2)	178.0(9)
Ag–Mn(2)–C(6)	148.1(4)	Mn(1)–C(3)–O(3)	178.2(9)
P(2)–Mn(2)–C(4)	91.8(4)	Mn(2)–C(4)–O(4)	177.7(9)
P(2)–Mn(2)–C(6)	91.0(4)	Mn(2)–C(5)–O(5)	178.4(12)
C(4)–Mn(2)–C(5)	91.9(5)	Mn(2)–C(6)–O(6)	178.0(12)

<sup>a</sup> Primed atoms are related to the unprimed ones by the transformation  $l - x, -y, -z$ .

exhibited by single Mn–Mn bonds in this type of carbonyl complex (ca. 2.90–3.10 Å). Therefore, it is expected that this intermetallic interaction is mainly accomplished through a bridging hydride (see below). In 5 there are three distinct Mn–Ag distances. The shortest Mn(2)–Ag distance (2.751(2) Å) can be considered as a normal single bond between these atoms (for example, a value of 2.664(2) Å has been found in  $[\text{Cp}(\text{CO})_2\text{Mo}(\mu\text{-AgPPh}_3)(\mu\text{-PPh}_2)\text{Mn}(\text{CO})_4]$ ).<sup>10</sup> The Mn(1)–Ag' (2.902(2) Å) and especially the Mn(1)–Ag (3.050(2) Å) separations are rather long and probably indicative of a weak interaction. Interestingly, comparable Mn–Ag distances (2.9929(1) and 2.961(1) Å) have been found in  $[\text{Mn}_2(\mu\text{-H})_2(\mu\text{-Ag}(\text{OCIO}_3)(\text{PPh}_3))(\text{CO})_6(\mu\text{-dppm})]$ , a compound which in solution easily dissociates a molecule of  $[\text{Ag}(\text{OCIO}_3)(\text{PPh}_3)]$ .<sup>11</sup>

(10) Horton, A. D.; Mays, M. J.; Adatia, T.; Henrick, K.; McPartlin, M. *J. Chem. Soc., Dalton Trans.* 1988, 1683.

(11) Carreño, R.; Riera, V.; Ruiz, M. A.; Bois, C.; Jeannin, Y. *Organometallics* 1992, 11, 2923.

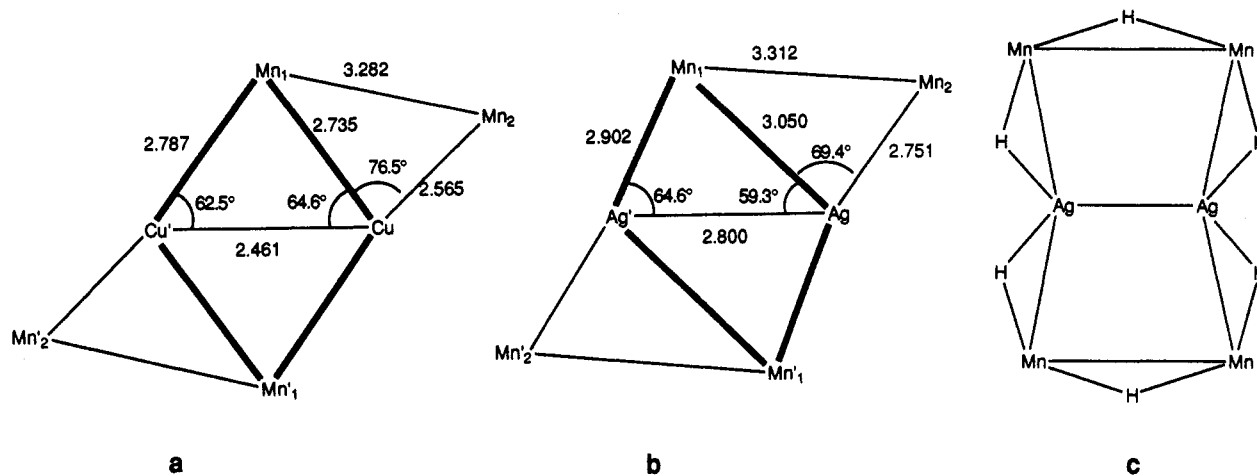


**Figure 2.** Bond lengths and angles in the metal cores of compounds **2** (a) and **5** (b). Part c represents a hypothetical distortion of these cores (see text).

The Ag-Ag distance in **5** (2.800(2) Å) is shorter than that found in metallic silver (2.883 Å).<sup>12</sup> It is also shorter than those found in the "raft" heterometallic clusters [Ag<sub>3</sub>M<sub>3</sub>(CO)<sub>12</sub>(Me<sub>2</sub>PCH<sub>2</sub>CH<sub>2</sub>PMe<sub>2</sub>)] (2.8424(5) Å for M = Nb, 2.8418(8) Å for M = Ta),<sup>13a,b</sup> [Ag<sub>3</sub>Co<sub>3</sub>{CN-(C<sub>6</sub>H<sub>3</sub>Me<sub>2</sub>)<sub>3</sub>}<sub>12</sub>] (2.825(1)-2.857(1) Å),<sup>13c</sup> and [Ag<sub>3</sub>Rh<sub>3</sub>Hg-(tripod)<sub>3</sub>]<sup>3+</sup> (2.968(4)-2.998(4) Å).<sup>5</sup> Even though an accurate location of the hydrides was not possible, there is substantial evidence (see Experimental Section) that four of them bridge Ag-Mn edges and two triply bridge the Mn<sub>2</sub>Ag faces. As will be discussed next, NMR data are only in partial agreement with the above locations.

The NMR data for **5** are not the expected ones, considering the crystal structure. Actually, the spectra indicate the chemical equivalence of all the Mn centers over the entire range of temperatures analyzed (298-183 K). Thus, the <sup>31</sup>P NMR spectra showed a single resonance at ca. 171 ppm. In agreement with this, the <sup>1</sup>H NMR spectra showed just two hydrido resonances at ca. -8 and -25 ppm (relative intensity 2:1). These chemical shifts are similar to those for the copper cluster **2**;<sup>1</sup> therefore, the positions of the hydride ligands should not differ greatly in these two compounds.

The couplings of the hydrido resonances of compound **5** have been identified by comparison of its <sup>1</sup>H and <sup>1</sup>H{<sup>31</sup>P} NMR spectra (Figure 3). At 250 K, the low-field resonance can be interpreted as arising from an AA'XX' spin system (A = <sup>1</sup>H, X = <sup>31</sup>P, J<sub>HP</sub> + J<sub>HP'</sub> = 42 Hz) with a further splitting of 105 Hz due to coupling with a single silver atom<sup>14</sup> (Figure 3f). This is confirmed by the corresponding <sup>1</sup>H{<sup>31</sup>P} spectrum (Figure 3e), which shows an apparent doublet (J<sub>HAg</sub> = 105 Hz; see below). At the same temperature, the high-field resonance appears as a broad, ill-resolved triplet of triplets (J<sub>HP</sub> = 26 Hz, J<sub>HAg</sub> = 12 Hz) which becomes a broad triplet (J<sub>HAg</sub> = 12 Hz) on <sup>31</sup>P decoupling. The chemical shifts and H-P and H-Ag coupling constants in the above hydrido resonances are

(12) Wells, A. F. *Structural Inorganic Chemistry*, 5th ed.; Clarendon Press: Oxford, U.K., 1984.

(13) (a) Calderazzo, F.; Pampaloni, G.; Englert, U.; Strähle, J. *Angew. Chem., Int. Ed. Engl.* 1989, 28, 471. (b) *J. Organomet. Chem.* 1990, 383, 45. (c) Leach, P. A.; Geib, S. J.; Cooper, N. J. *Organometallics* 1992, 12, 4367.

(14) The true situation is much more complicated, as three different spin systems can be identified, considering the different isotopomers present. However, the fact that the broadness of the resonances precludes the distinction between similar couplings (e.g. <sup>1</sup>J<sub>H<sup>109</sup>Ag</sub> or <sup>1</sup>J<sub>H<sup>107</sup>Ag</sub>) or the observation of small ones (perhaps J<sub>HP</sub> or <sup>2</sup>J<sub>HAg</sub>) considerably simplifies the appearance of the spectrum.

comparable to those observed for the trinuclear cluster [Mn<sub>2</sub>(μ-AgPPh<sub>3</sub>)(μ-H)<sub>3</sub>(CO)<sub>6</sub>(μ-tedip)] (<sup>1</sup>J<sub>HAg</sub> = 72 Hz; <sup>2</sup>J<sub>HAg</sub> = 24 Hz).<sup>1</sup> High values (60-110 Hz) are usually also found for one-bond H-Ag couplings in heterometallic complexes having μ<sub>2</sub>-H(MAg) moieties (M = transition metal).<sup>5,15</sup> All the previous evidence makes the assignment of the -8 and -25 ppm resonances in **5** (to Mn-H-Ag and Mn-H-Mn bridging hydrido atoms, respectively; Chart 2) reasonable. This is in agreement with the X-ray location of the H atoms in **5** (Figure 1), except that there μ<sub>3</sub>-H (at Mn<sub>2</sub>Ag faces) rather than μ<sub>2</sub>-H (at Mn<sub>2</sub> edges) positions are suggested. Unfortunately, our NMR data are not completely conclusive in this respect. In fact, although the low value of the H-Ag coupling (12 Hz) for the -25 ppm resonance is best interpreted as resulting from a two-bond pathway connection (and hence as due to a μ<sub>2</sub>-H(Mn<sub>2</sub>) atom, in agreement with the low chemical shift) <sup>1</sup>J<sub>HAg</sub> values for μ<sub>3</sub>-H ligands can be also quite low (for example ca. 30 Hz in clusters of the type [Ag<sub>2</sub>Ru<sub>4</sub>(μ<sub>3</sub>-H)<sub>2</sub>(CO)<sub>12</sub>L<sub>2</sub>]; L = phosphine, diphosphine).<sup>16</sup>

The NMR spectra of **5** at 250 K or below require the presence of a plane of symmetry relating atoms which are not equivalent in the solid state (for example, X(1) and X(2); X = Mn, H, P). This can be explained if a fluxional process (Figure 4) similar to the one postulated<sup>1</sup> for the copper cluster **2** is assumed. The proposed process requires the cleavage of the Mn(1)-Ag bond in the transition state (yielding a structure similar to that shown in Figure 2c). As we have previously discussed, this is the longest Mn-Ag distance in the cluster, and its cleavage should then imply the lowest energetic cost. On the other hand, it has been found in some instances that fluxional processes are faster for silver than for related copper heterometallic clusters.<sup>16a</sup> Thus, the combination of these two facts could perhaps explain why the fluxional process is easily slowed down (so as to observe the "static spectrum") for the copper cluster **2** but not for the silver analogue **5**.

However, the variable-temperature <sup>1</sup>H{<sup>31</sup>P} NMR spectra of **5** clearly indicate that the situation is more complex above 250 K (Figure 3a-e). In fact, as the temperature is

(15) (a) Pt(μ-H)Ag complexes: Albinati, A.; Chaloupka, S.; Demartin, F.; Koetzle, T. F.; Rüeger, H.; Venanzi, M.; Wolfer, M. K. *J. Am. Chem. Soc.* 1993, 115, 169 and references therein. (b) Ir(μ-H)Ag complexes: Albinati, A.; Auklin, C.; Janser, P.; Lehner, H.; Matt, D.; Pregosin, P. S.; Venanzi, L. *Inorg. Chem.* 1989, 28, 1105.

(16) (a) Freeman, M. J.; Orpen, A. G.; Salter, I. D. *J. Chem. Soc., Dalton Trans.* 1987, 379. (b) Brown, S. S. D.; Salter, I. D.; Toupet, L. *J. Chem. Soc., Dalton Trans.* 1988, 757.

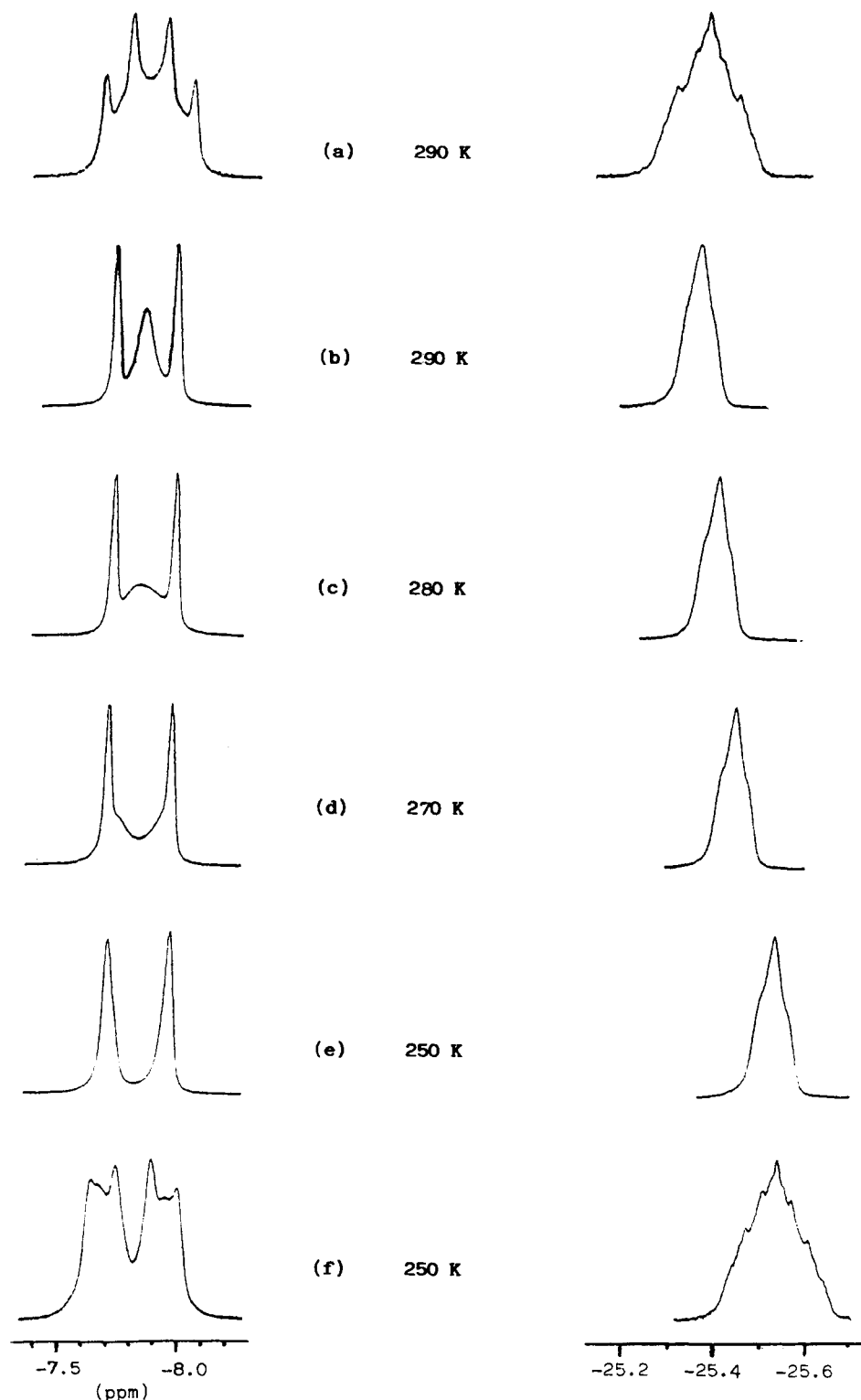


**Figure 3.** Variable-temperature 400.13-MHz  $^1\text{H}$  NMR spectra of **5** in  $\text{CD}_2\text{Cl}_2$  solution: (a and f) normal  $^1\text{H}$  spectra; (b–e)  $^1\text{H}\{^{31}\text{P}\}$  spectra.

increased, the apparent doublet at *ca.* -8 ppm adopts shapes which are characteristic of  $\text{AA}'\text{XX}'$  systems (now  $\text{A} = ^1\text{H}$ ,  $\text{X} = \text{Ag}$ ). Therefore, the separation between the strongest lines, which remains 105 Hz, must correspond to  $J_{\text{HAg}} + J_{\text{H'Ag}}$ . Moreover, the change in shape of the multiplet from low to room temperature (while  $J_{\text{HAg}} + J_{\text{H'Ag}}$  is kept constant) requires a modification of the individual values of the coupling constants involved (H–Ag and Ag–Ag couplings). We interpret this as evidence that fast structural rearrangements, different from the one just discussed, are taking place and yield averaged

structures (and then couplings) which are temperature-dependent. Unfortunately, our data do not allow us to advance any sound proposal to account for these observations.

**Reaction with  $[\text{Ac}(\text{C}\equiv\text{CPh})]_n$ .** As with the silver or copper alkynyls, dihydride **1** reacts smoothly at room temperature with  $[\text{Au}(\text{C}\equiv\text{CPh})]_n$  to give a mixture of the alkynyl complex **4** and, unexpectedly, a violet species, characterized by an X-ray study as the pentanuclear hydrido cluster  $[\text{AuMn}_4(\mu\text{-H})_5(\text{CO})_{12}(\mu\text{-tedip})_2]$  (**6**).

The structure of **6** is depicted in Figure 5 together with

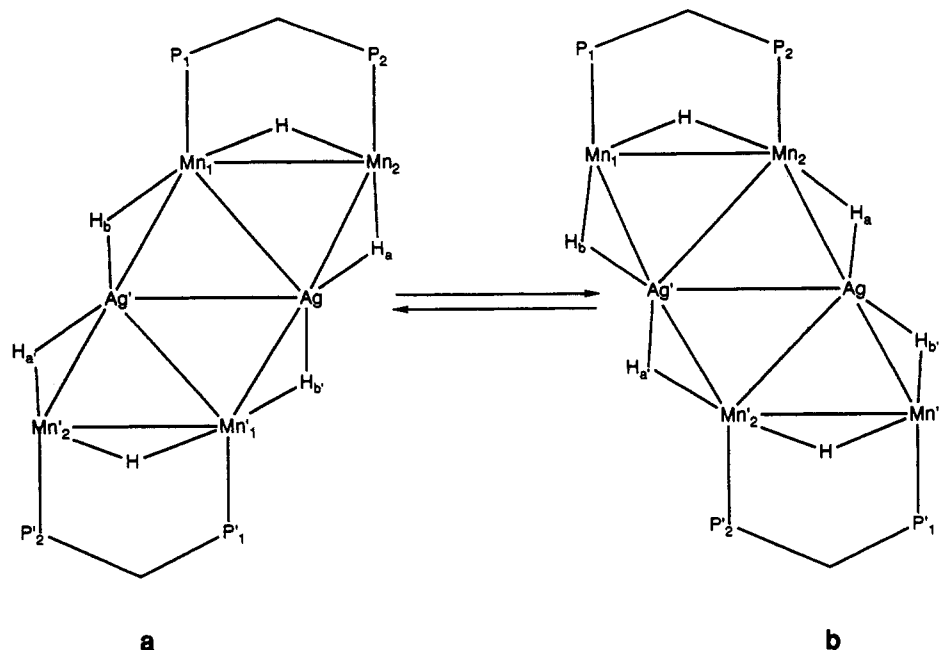


**Figure 4.** Schematic view of the fluxional rearrangement proposed for compound **5** in solution below *ca.* 250 K.

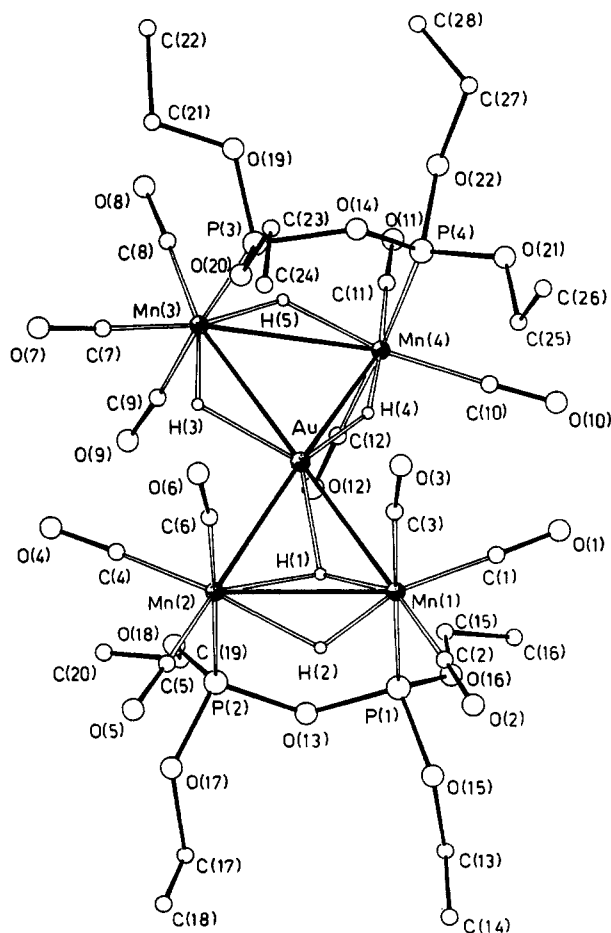


**Figure 5.** Molecular structure of  $[\text{AuMn}_4(\mu\text{-H})_5(\text{CO})_{12}\{\mu\text{-tedip}\}_2]$  (**6**) with the atom-numbering scheme. The positions of the hydrides could not be established unambiguously.

the atom-numbering scheme. A summary of the important bond distances and angles is given in Table 3. The metal core consists of two  $\text{Mn}_2\text{Au}$  triangles sharing a common Au vertex (*i.e.* a "bow tie" type) and tilted by  $21.1(1)^\circ$ . Concerning the hydrido ligands, there is evidence (see Experimental Section) that two of them bridge Mn–Mn

edges, two others bridge Mn–Au edges, and one triply bridges a  $\text{Mn}_2\text{Au}$  triangle. The intermetallic distances deserve comment. Three of the Mn–Au bond lengths are very similar (around 2.84 Å), whereas Mn(2)–Au is significantly shorter (2.771(2) Å). These values are in the range found for the Mn–Au cluster  $[\text{Mn}_2(\mu\text{-AuPPh}_3)_2(\mu\text{-H})(\text{CO})_6(\mu\text{-dppm})]\text{PF}_6$  (2.845(3) Å and 2.767(4) Å for the Mn–Au, hydride-bridged edges).<sup>11</sup> In contrast, in related compounds with Mn–Au edges lacking bridging hydrides, significantly shorter distances are found, irrespective of the electronic unsaturation of the cluster (averaged values: 2.660(3) and 2.652(2) Å, respectively, for  $[\text{Mn}_2(\mu\text{-AuPPh}_3)(\mu\text{-X})(\text{CO})_6(\mu\text{-tedip})]$  with X = Br,<sup>17</sup> or H;<sup>1</sup> 2.684(4) Å for the unbridged Mn–Au edge in  $[\text{Mn}_2(\mu\text{-AuPPh}_3)_2(\mu\text{-H})(\text{CO})_6(\mu\text{-dppm})]\text{PF}_6$ .<sup>11</sup> Thus, the relatively short value of the Mn(2)–Au distance could perhaps be indicative of a true asymmetry in the coordination of H(1) (close to an edge-bridging position over the Au–Mn(1) edge). The two Mn–Mn separations differ more significantly. Thus, the value of this distance in the triangle with three hydrides (3.080(2) Å) is consistent with a single Mn–Mn bond order (for example, it is 3.090(3) Å in  $[\text{Mn}_2(\mu\text{-AuPPh}_3)(\mu\text{-Br})(\text{CO})_6(\mu\text{-tedip})]$ <sup>17</sup> or 3.0661(8) Å in  $[\text{Mn}_2(\mu\text{-AuPPh}_3)(\mu\text{-PPh}_2)(\text{CO})_6]$ .<sup>18</sup> In contrast, the Mn(1)–Mn(2) distance (2.860(2) Å) is much shorter and almost identical with that found in the unsaturated cationic complex  $[\text{Mn}_2(\mu\text{-AuPPh}_3)_2(\mu\text{-H})(\text{CO})_6(\mu\text{-dppm})]^+$  (2.863(5) Å),<sup>11</sup> although it is still longer than that in the unsaturated trinuclear cluster  $[\text{Mn}_2(\mu\text{-AuPPh}_3)(\mu\text{-H})(\text{CO})_6(\mu\text{-tedip})]$  (2.739(3) Å).<sup>1</sup> Thus, the electronic deficiency of **6** (two electrons, by considering the EAN rule) seems to be mainly located on the Mn(1)–Mn(2) bond.

Crystallographically characterized clusters in which a four-coordinated gold(I) center connects two polynuclear fragments are scarce,<sup>19</sup> and to our knowledge compound **6** is the first in this class which has hydrido ligands bonded

(17) Riera, V.; Ruiz, M. A.; Tiripicchio, A.; Tiripicchio-Camellini, M. *J. Chem. Soc., Dalton Trans.* 1987, 1551.

(18) Iggo, J. A.; Mays, M. J.; Raithby, P. R.; Henrick, K. *J. Chem. Soc., Dalton Trans.* 1984, 633.

(19) Draper, S. M.; Housecroft, C. E.; Rees, J. E.; Shongwe, M. S.; Haggerty, B. S.; Rheingold, A. L. *Organometallics* 1992, 11, 2356 and references therein.

**Table 3. Important Interatomic Distances (Å) and Angles (deg) for Compound 6**

Au-Mn(1)	2.841(2)	P(1)-O(15)	1.599(11)
Au-Mn(2)	2.771(2)	P(1)-O(16)	1.498(12)
Au-Mn(3)	2.837(2)	P(2)-O(13)	1.628(10)
Au-Mn(4)	2.839(2)	P(2)-O(17)	1.591(12)
Mn(1)-Mn(2)	2.860(2)	P(2)-O(18)	1.637(18)
Mn(3)-Mn(4)	3.080(2)	P(3)-O(14)	1.625(10)
Mn(1)-P(1)	2.226(3)	P(3)-O(19)	1.570(9)
Mn(2)-P(2)	2.212(4)	P(3)-O(20)	1.549(8)
Mn(3)-P(3)	2.221(3)	P(4)-O(14)	1.600(8)
Mn(4)-P(4)	2.209(3)	P(4)-O(21)	1.566(12)
Mn(1)-C(1)	1.775(13)	P(4)-O(22)	1.575(9)
Mn(1)-C(2)	1.788(11)	C(1)-O(1)	1.164(16)
Mn(1)-C(3)	1.819(11)	C(2)-O(2)	1.146(14)
Mn(2)-C(4)	1.823(14)	C(3)-O(3)	1.119(14)
Mn(2)-C(5)	1.745(11)	C(4)-O(4)	1.157(18)
Mn(2)-C(6)	1.842(11)	C(5)-O(5)	1.171(14)
Mn(3)-C(7)	1.783(13)	C(6)-O(6)	1.130(14)
Mn(3)-C(8)	1.746(10)	C(7)-O(7)	1.147(17)
Mn(3)-C(9)	1.829(12)	C(8)-O(8)	1.185(13)
Mn(4)-C(10)	1.821(16)	C(9)-O(9)	1.134(15)
Mn(4)-C(11)	1.772(12)	C(10)-O(10)	1.127(21)
Mn(4)-C(12)	1.825(11)	C(11)-O(11)	1.155(15)
P(1)-O(13)	1.631(10)	C(12)-O(12)	1.140(14)
Mn(1)-Au-Mn(2)	61.3(1)	Mn(1)-P(1)-O(15)	113.4(5)
Mn(1)-Au-Mn(4)	119.9(1)	Mn(1)-P(1)-O(16)	120.3(6)
Mn(2)-Au-Mn(3)	115.1(1)	O(13)-P(1)-O(15)	102.0(6)
Mn(3)-Au-Mn(4)	65.7(1)	O(13)-P(1)-O(16)	101.9(6)
Au-Mn(1)-Mn(2)	58.2(1)	O(15)-P(1)-O(16)	101.3(7)
Au-Mn(1)-P(1)	103.1(1)	Mn(2)-P(2)-O(13)	118.1(4)
Au-Mn(1)-C(1)	95.1(4)	Mn(2)-P(2)-O(17)	114.4(6)
Au-Mn(1)-C(3)	76.9(4)	Mn(2)-P(2)-O(18)	112.6(6)
Mn(2)-Mn(1)-P(1)	91.3(1)	O(13)-P(2)-O(17)	101.1(7)
Mn(2)-Mn(1)-C(2)	115.6(4)	O(13)-P(2)-O(18)	100.4(6)
Mn(2)-Mn(1)-C(3)	89.6(4)	O(17)-P(2)-O(18)	108.7(9)
P(1)-Mn(1)-C(1)	88.8(4)	Mn(3)-P(3)-O(14)	117.6(3)
P(1)-Mn(1)-C(2)	90.6(4)	Mn(3)-P(3)-O(19)	119.9(4)
C(1)-Mn(1)-C(2)	91.9(5)	Mn(3)-P(3)-O(20)	114.1(4)
C(1)-Mn(1)-C(3)	90.2(5)	O(14)-P(3)-O(19)	94.3(5)
C(2)-Mn(1)-C(3)	89.6(5)	O(14)-P(3)-O(20)	101.8(5)
Au-Mn(2)-Mn(1)	60.6(1)	O(19)-P(3)-O(20)	106.2(5)
Au-Mn(2)-P(2)	99.8(1)	Mn(4)-P(4)-O(14)	115.4(3)
Au-Mn(2)-C(4)	90.1(4)	Mn(4)-P(4)-O(21)	121.9(4)
Au-Mn(2)-C(6)	81.9(4)	Mn(4)-P(4)-O(22)	114.0(4)
Mn(1)-Mn(2)-P(2)	89.5(1)	O(14)-P(4)-O(21)	99.7(5)
Mn(1)-Mn(2)-C(5)	116.0(4)	O(14)-P(4)-O(22)	103.6(5)
Mn(1)-Mn(2)-C(6)	92.7(4)	O(21)-P(4)-O(22)	99.4(5)
P(2)-Mn(2)-C(4)	88.8(4)	P(1)-O(13)-P(2)	125.1(6)
P(2)-Mn(2)-C(5)	90.8(4)	P(3)-O(14)-P(4)	128.4(6)
C(4)-Mn(2)-C(5)	94.1(6)	P(1)-O(15)-C(13)	127.0(14)
C(4)-Mn(2)-C(6)	89.7(5)	P(1)-O(16)-C(15)	134.2(15)
C(5)-Mn(2)-C(6)	87.6(6)	P(2)-O(17)-C(17)	130.1(19)
Au-Mn(3)-P(3)	91.7(1)	P(2)-O(18)-C(19)	137.1(16)
Au-Mn(3)-C(7)	109.1(4)	P(3)-O(19)-C(21)	120.9(11)
Au-Mn(3)-C(9)	84.6(4)	P(3)-O(20)-C(23)	121.8(10)
P(3)-Mn(3)-C(7)	90.6(4)	P(4)-O(21)-C(25)	122.4(11)
P(3)-Mn(3)-C(8)	93.1(4)	P(4)-O(22)-C(27)	123.3(10)
C(7)-Mn(3)-C(8)	92.9(6)	Mn(1)-C(1)-O(1)	179.5(10)
C(7)-Mn(3)-C(9)	90.4(6)	Mn(1)-C(2)-O(2)	178.0(11)
C(8)-Mn(3)-C(9)	90.4(6)	Mn(1)-C(3)-O(3)	173.4(10)
Au-Mn(4)-P(4)	100.4(1)	Mn(2)-C(4)-O(4)	176.6(11)
Au-Mn(4)-C(10)	108.0(5)	Mn(2)-C(5)-O(5)	177.3(11)
Au-Mn(4)-C(12)	74.0(4)	Mn(2)-C(6)-O(6)	173.1(11)
P(4)-Mn(4)-C(10)	91.2(4)	Mn(3)-C(7)-O(7)	176.0(11)
P(4)-Mn(4)-C(11)	91.9(4)	Mn(3)-C(8)-O(8)	177.9(11)
C(10)-Mn(4)-C(11)	92.2(6)	Mn(3)-C(9)-O(9)	175.9(11)
C(10)-Mn(4)-C(12)	93.1(6)	Mn(4)-C(10)-O(10)	177.5(13)
C(11)-Mn(4)-C(12)	92.4(6)	Mn(4)-C(11)-O(11)	177.9(12)
Mn(1)-P(1)-O(13)	115.5(3)	Mn(4)-C(12)-O(12)	177.2(11)

to the gold atom. Compound 6 can be related with the anionic clusters  $[\{\text{Os}_3(\mu\text{-H})(\text{CO})_{10}\}_2\text{M}]^-$  ( $\text{M} = \text{Au},^{20} \text{Ag}^{21}$ ). However, the latter have a four-electron deficiency (also located between the osmium atoms bonded to the group 11 metal atom) and exhibit a planar  $\text{Os}_4\text{M}$  central moiety. In contrast, the dihedral angle between  $\text{Mn}_2\text{Au}$  planes in 6 is  $21.1(1)^\circ$ . A closer structural similarity is found between

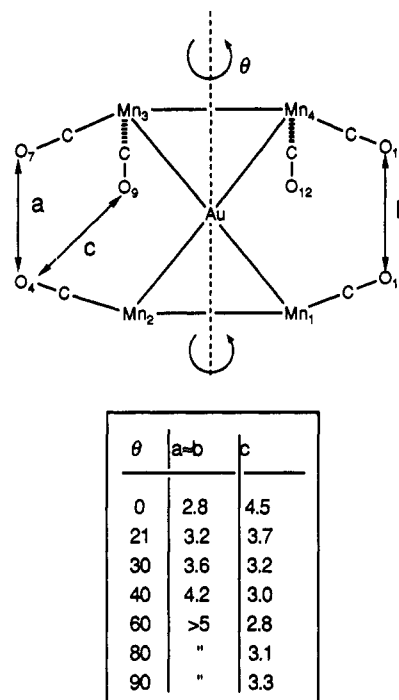


**Figure 6.** Schematic representation of the main interatomic contacts involving both dimanganese moieties in cluster 6 and their calculated dependence on the dihedral angle ( $\theta$ ) between  $\text{Mn}_2\text{Au}$  planes (values for  $\theta = 21^\circ$  are those actually measured in the X-ray study).

6 and the isoelectronic anion  $[\text{Re}_4\text{Pt}(\mu\text{-H})_5(\text{CO})_{16}]^-$ .<sup>22</sup> The rhenium cluster exhibited a dihedral angle between  $\text{Re}_2\text{-Pt}$  planes of  $36.3^\circ$  (but  $0^\circ$  in its protonated form). However, the electron deficiency of this cluster seems to be more delocalized than in 6, as judged from the observed intermetallic lengths.

There has been some discussion about the causes which determine the value of the dihedral angle in this class of "bow tie" clusters. Crystal packing and steric effects seem to be the favored explanation,<sup>19,22</sup> although electronic factors are also suspected to influence the final geometry.<sup>22</sup> Examination of the interatomic contacts in 6 reveals that the greater repulsive interactions between atoms belonging to different dimanganese units must be those between the carbonyl oxygen atoms  $\text{O}(4)\cdots\text{O}(7)$  and  $\text{O}(1)\cdots\text{O}(10)$  ( $a$  and  $b$  in Figure 6). The observed values (3.24(1) and 3.20(1) Å) are only slightly higher than twice the van der Waals radius for oxygen (3.0 Å).<sup>23</sup> However, these contacts are very sensitive to the dihedral angle ( $\theta$ ) between both metal planes (Figure 6). We have estimated these changes by rotating the  $\text{AuMn}(3)\text{Mn}(4)$  moiety around the axis going through Au and the midpoint of the  $\text{Mn}(1)\text{Mn}(2)$  vector. Values for  $a$  and  $b$  changed similarly between 0 and  $90^\circ$ , and an average value has been collected in Figure 6. Thus, with the experimental angle of  $\theta = 21^\circ$  as a starting point, both  $a$  and  $b$  decrease on approaching  $\theta = 0^\circ$  and increase toward  $\theta = 90^\circ$ . Then, on this basis alone, we would have expected a value of  $\theta = 90^\circ$  for 6, very different from its

(20) Johnson, B. F. G.; Kaner, D. A.; Lewis, J.; Raithby, P. R. *J. Chem. Soc., Chem. Commun.* 1981, 753.

(21) Fajardo, M.; Gómez-Sal, M. P.; Holden, H. D.; Johnson, B. F. G.; Lewis, J.; McQueen, R. C. S.; Raithby, P. R. *J. Organomet. Chem.* 1984, 267, C25.

(22) Ciani, G.; Moret, M.; Sironi, A.; Antognazza, P.; Beringhelli, T.; D'Alfonso, G.; Della Pergola, R.; Minoja, A. *J. Chem. Soc., Chem. Commun.* 1991, 1255.

(23) Bondi, A. *J. Phys. Chem.* 1964, 68, 441.

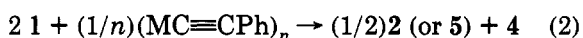
actual value in the crystal. However, as we increase  $\theta$ , a new repulsion emerges, that between O(4) and O(9) ( $c$  in Figure 6). This new repulsion is maximum (minimum distance *ca.* 2.8 Å) around  $\theta = 60^\circ$  and becomes low again at  $\theta = 90^\circ$ .

Therefore, with our simplified model we conclude that, in order to keep the repulsion between the dimanganese moieties in **6** at a minimum (O...O contacts above 3.0 Å),  $\theta$  values either close to  $90^\circ$  or in the range  $20\text{--}40^\circ$  are both satisfactory. We suspect that the fact that the experimental value of  $\theta$  (*ca.*  $21^\circ$ ) in cluster **6** is the lowest attainable without imposing excessive interatomic repulsion between the dimanganese moieties reflects a tendency to the planar ( $\theta = 0^\circ$ ) core geometry. This presumably has an electronic (bonding) origin, as has been suggested for the above-mentioned  $\text{Re}_4\text{Pt}$  clusters.<sup>22</sup>

Spectroscopic data in solution (Table 1 and Experimental Section) for compound **6** are not consistent with the solid-state structure. The IR spectrum in petroleum ether exhibits nine  $\nu(\text{CO})$  stretching bands. This indicates that, at least, the two dimanganese moieties of the molecule are not equivalent in solution (itself consistent with the crystal structure). In contrast with this, however, the  $^{31}\text{P}$  NMR spectrum of **6** displays a single resonance from  $+25$  to  $-90^\circ\text{C}$ . Therefore, it is clear that there must be a dynamic process equalizing the chemical environments of all four manganese atoms. The  $^1\text{H}$  NMR spectrum of **6** did not show significant changes in the mentioned range of temperatures either. It exhibits a quintet at *ca.*  $-7.6$  ppm and a triplet at *ca.*  $-19.3$  ppm. The chemical shift and P-H coupling of the latter are typical of hydrido ligands bridging manganese atoms, and the less shielded resonance corresponds to the three hydrido ligands bridging Mn and Au atoms. The observed P-H coupling (10 Hz) in the latter must be regarded as low,<sup>1,11</sup> but it is obviously an averaged value.

In order to reconcile the  $^{31}\text{P}$  and  $^1\text{H}$  NMR spectra of **6** with the main features of the solid-state structure, we propose that a scrambling of the hydrido ligands involved in bonding with the gold atom is taking place in solution (Figure 7). For simplicity, we have assumed a planar metal core in solution. Although this is not unlikely, given the relatively low dihedral angle in the crystal, in the same way we could include a slight tilting of the metal core in our proposal so as to keep the solution structures identical with the solid-state one. It can be clearly seen from Figure 7 that interconversion between structures **a-f** effectively averages the chemical environments of H(1), H(3), and H(4) on one hand as well as those of H(2) and H(5) on the other, in addition to those of manganese and phosphorus atoms of the molecule. This also implies that, on a time average, the electronic unsaturation of the cluster should be equally distributed between both dimanganese moieties.

**Reaction Pathways Leading to Clusters 2, 5, and 6.** The reaction between copper(I) halides and **1** to give the  $\text{Mn}_4\text{Cu}_2$  cluster **2** (eq 1) seems at first sight somewhat casual. It was then surprising that the copper and silver alkynyls reacted with **1**, following exactly the same type of stoichiometry (eq 2).



This behavior is not usual for the polymeric group 11 alkynyls. Usually, when they react with transition-metal complexes to give heterometallic derivatives, both the alkynyl group and the group 11 metal atom are incorpo-

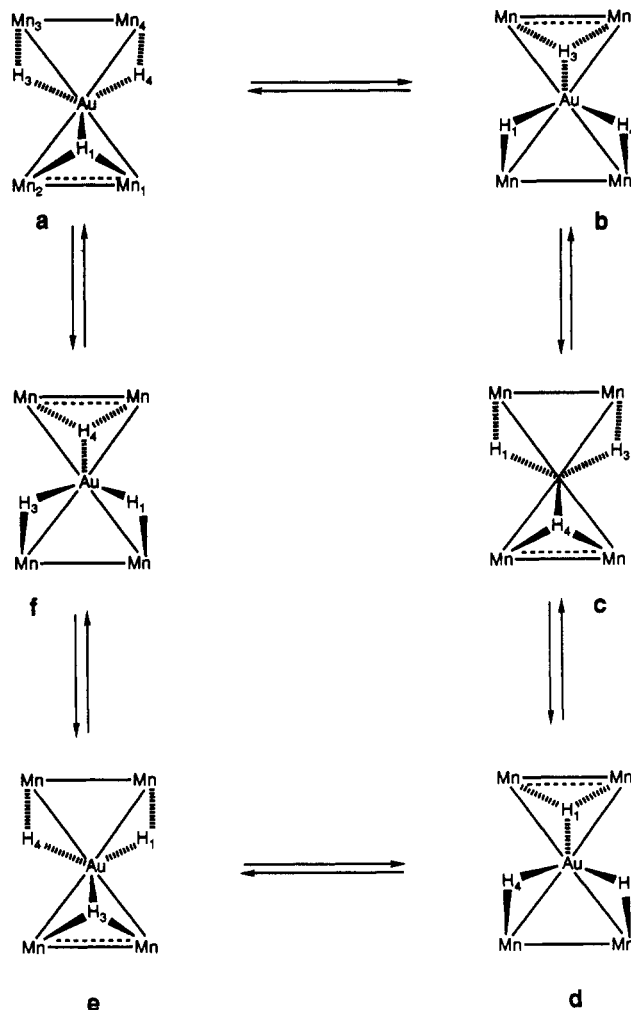
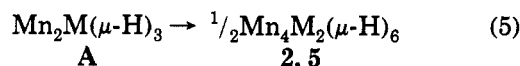
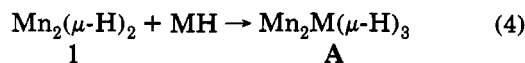
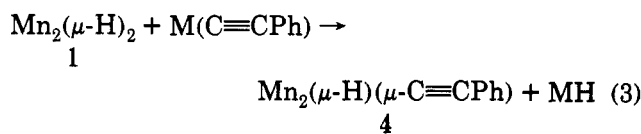


**Figure 7.** Schematic view of the scrambling process proposed for the hydrido ligands in compound **6**.

ated in the same reaction product.<sup>24</sup> In contrast, in our reactions the entering reagent is distributed among two reaction products (the group 11 metal atom in one, the alkynyl group or halide in the other), thus suggesting a complex mechanism. The formation of a transient species seems reasonable in order to facilitate the necessary atom transfer. Such a species could be the corresponding group 11 metal hydride, as shown in the following sequence (eqs 3–5;  $\text{Mn}_2$  refers to the  $\text{Mn}_2(\text{CO})_6(\mu\text{-tedip})$  moiety). Equa-



tion 3 mimics the well-known reaction between **1** (or its *dppm* analogue) and protonic acids ( $\text{HX}$ ;  $\text{X} = \text{Cl}^-$ ,  $\text{SR}^-$ ,  $\text{RCO}_2^-$ ), which results in the formation of the corresponding  $\text{Mn}_2(\mu\text{-H})(\mu\text{-X})$  species and intermolecular elimination of

(24) Espinet, P.; Fornies, J.; Martínez, F.; Tomás, M.; Lalinde, E.; Moreno, M. T.; Ruiz, A.; Welch, A. *J. Chem. Soc., Dalton Trans.* 1990, 791 and references therein.



$C_6F_5$ , Ph),<sup>29</sup> although in alkenyl complexes  $H_\alpha$  is more commonly found to display the highest chemical shift.<sup>8,30</sup> On the other hand, although the resonances of the alkenylic protons in 7 and 8 were only moderately broad ( $w_{1/2} = 5\text{--}11$  Hz), they showed no indication of H–H or H–P coupling. Thus, it would be tempting to assume a *cis* relative arrangement of these atoms, because *trans* alkenylic protons usually display large mutual couplings (usually 14–16 Hz<sup>8,29,30b-d</sup>) which should be visible even for our broad resonances. However, NOE difference spectra measured for compound 8 suggest that these protons are actually in a relative *trans* arrangement. Thus, irradiation of the 5.7 ppm resonance ( $H_\alpha$ ) caused a significant enhancement for the <sup>t</sup>Bu resonance but not for that of  $H_\beta$ . Analogously, irradiation of the 6.7 ppm resonance ( $H_\beta$ ) enhanced the <sup>t</sup>Bu resonance but not that for  $H_\alpha$ . Although usually large, *trans* H–H coupling in substituted alkenes can be reduced by the presence of some substituents.<sup>31</sup> Then, the combination of the moderate broadness of the resonances and the electronic influence of the metal center can perhaps explain our inability to observe any H–H couplings in these resonances.

The formation of clusters 7 and 8 from 1 and  $[Au(C\equiv CR)(PR'_3)]$  implies the addition of both hydrido atoms of 1 into the entering alkynyl group and migration of the  $Au(PR'_3)$  fragment up to the dimanganese center. This behavior then resembles that shown<sup>29</sup> by  $[Os_3(\mu-H)_2(CO)_{10}]$  toward  $[M(C\equiv CR)(PPh_3)]$  ( $M = Cu, Ag, Au$ ;  $R = C_6F_5, Ph$ ). In this case, it was proposed that an Au–C oxidative addition could perhaps occur as a first step, followed by migration of the hydrido ligands to the alkynyl group. However, the formation of alkenyl complexes from 1-alkynes and dihydrides  $[Mn_2(\mu-H)_2(CO)_6(\mu-dppm)]$ <sup>8</sup> and  $[Os_3(\mu-H)_2(CO)_{10}]$ <sup>32</sup> suggests that the first step in the formation of 7 and 8 might instead be the insertion of the gold alkynyl into one of the Mn–H–Mn bonds. Further steps would then accomplish the exchange of positions between the remaining hydrido atom and the gold phosphine fragment.

Silver or copper analogues of the clusters 7 and 8 could not be obtained by reaction of 1 with the alkynyl complexes  $[M(C\equiv CPh)(PPh_3)]$  ( $M = Cu, Ag$ ). Instead, these reactions led slowly to a generalized decomposition of the starting dihydride. Thus, the chemical differences between the heavier element of the group 11 triad and its lighter relatives are shown once more.

## Experimental Section

**General Considerations.** All reactions were carried out under a nitrogen atmosphere using standard Schlenk techniques. Solvents were purified according to standard literature procedures<sup>33</sup> and distilled under nitrogen prior to use. Petroleum ether refers to that fraction distilling in the range 60–65 °C. The

**Table 4. Experimental Data for the X-ray Diffraction Studies**

	compd 5	compd 6
mol formula	$C_{28}H_{46}Ag_2Mn_4O_{22}P_4$	$C_{28}H_{45}AuMn_4O_{22}P_4$
mol wt	1294.04	1274.26
cryst syst	triclinic	triclinic
space group	$P\bar{1}$	$P\bar{1}$
radiatn	Nb-filtered Mo K $\alpha$ ( $\lambda = 0.71073 \text{ \AA}$ )	
<i>a</i> , Å	14.014(9)	18.356(7)
<i>b</i> , Å	9.272(7)	11.952(5)
<i>c</i> , Å	10.741(6)	11.688(5)
$\alpha$ , deg	102.91(2)	74.37(2)
$\beta$ , deg	107.01(2)	78.86(2)
$\gamma$ , deg	103.37(2)	83.42(2)
<i>V</i> , Å <sup>3</sup>	1233(1)	2418(2)
<i>Z</i>	1	2
<i>D</i> <sub>calcd</sub> , g cm <sup>-3</sup>	1.742	1.750
<i>F</i> (000)	644	1256
cryst dimens, mm	0.25 × 0.30 × 0.35	0.20 × 0.22 × 0.30
$\mu$ (Mo K $\alpha$ ), cm <sup>-1</sup>	19.21	41.93
$2\theta$ range, deg	6–54	6–50
rlins measd	$\pm h, \pm k, l$	$\pm h, \pm k, l$
no. of unique total data	5403	8561
no. of unique obsd data	3027 ( $I > 2\sigma(I)$ )	5266 ( $I > 2\sigma(I)$ )
<i>R</i>	0.0547	0.0433
<i>R</i> <sub>w</sub>	0.0622	0.0471

**Table 5. Fractional Atomic Coordinates ( $\times 10^4$ ) and Isotropic Thermal Parameters ( $\text{\AA}^2 \times 10^4$ ) with Esd's in Parentheses for the Non-Hydrogen Atoms of Complex 5**

	<i>x/a</i>	<i>y/b</i>	<i>z/c</i>	<i>U</i>
Ag	4935(1)	-194(1)	-1356(1)	684(3) <sup>a</sup>
Mn(1)	3541(1)	1370(1)	-227(1)	561(4) <sup>a</sup>
Mn(2)	3572(1)	511(2)	-3376(1)	675(6) <sup>a</sup>
P(1)	2038(1)	-580(2)	-1181(2)	611(8) <sup>a</sup>
P(2)	2364(2)	-1702(3)	-3756(2)	753(11) <sup>a</sup>
O(1)	3336(6)	2128(10)	2482(8)	1188(41) <sup>a</sup>
O(2)	5580(5)	3877(8)	824(8)	997(34) <sup>a</sup>
O(3)	2462(6)	3615(8)	-922(10)	1236(49) <sup>a</sup>
O(4)	3559(7)	-530(12)	-6170(8)	1356(60) <sup>a</sup>
O(5)	5329(7)	3398(11)	-2637(11)	1365(52) <sup>a</sup>
O(6)	1927(8)	1963(12)	-4136(11)	1458(65) <sup>a</sup>
O(7)	1886(4)	-1883(6)	-2577(6)	745(25) <sup>a</sup>
O(8)	1703(4)	-1696(7)	-347(6)	755(27) <sup>a</sup>
O(9)	1037(4)	-45(7)	-1592(8)	931(32) <sup>a</sup>
O(10)	2636(11)	-3292(11)	-3917(12)	1703(82) <sup>a</sup>
O(11)	1353(7)	-1995(10)	-5045(8)	1389(47) <sup>a</sup>
C(1)	3418(6)	1803(10)	1410(10)	754(40) <sup>a</sup>
C(2)	4814(7)	2904(10)	426(9)	713(37) <sup>a</sup>
C(3)	2876(7)	2740(10)	-675(11)	841(45) <sup>a</sup>
C(4)	3573(8)	-88(14)	-5067(10)	927(48) <sup>a</sup>
C(5)	4654(9)	2297(15)	-2903(11)	963(57) <sup>a</sup>
C(6)	2576(8)	1424(13)	-3840(12)	967(55) <sup>a</sup>
C(7)	2327(8)	-2644(11)	158(10)	864(25)
C(8)	1679(10)	-3580(14)	827(13)	1153(36)
C(9)	-46(11)	-1136(16)	-2232(14)	1237(40)
C(10)	-776(13)	-293(19)	-2253(17)	1509(52)
C(11)	3292(25)	-3689(41)	-4599(33)	2606(131)
C(12)	3481(20)	-4827(30)	-4839(25)	2408(89)
C(13)	421(17)	-3338(25)	-5483(23)	1911(75)
C(14)	-112(13)	-3885(17)	-6887(17)	1358(47)

<sup>a</sup> Equivalent isotropic *U*, defined as one-third of the trace of the orthogonalized  $U_{ij}$  tensor.

compounds  $[Mn_2(\mu-H)_2(CO)_6(\mu-tedip)]$ ,<sup>1</sup>  $[M(C\equiv CPh)]_n$  ( $M = Cu$ ,<sup>34</sup>  $Ag$ ,<sup>35</sup>  $Au$ ,<sup>36</sup>) and  $[Au(C\equiv CR)(PR'_3)]$  ( $R = Ph$ ,  $R' = p\text{-tol}$ ;  $R = ^tBu$ ,  $R' = Ph$ )<sup>37</sup> were prepared according to literature procedures. Filtrations were carried out using diatomaceous earth. Alumina for column chromatography was deactivated by

(34) Van Koten, G.; Noltes, J. G. In *Comprehensive Organometallic Chemistry*; Wilkinson, G., Stone, F. G. A., Abel, E. W., Eds.; Pergamon Press: Oxford, U.K., 1982; Vol. 2, p 720.

(35) Van Koten, G.; Noltes, J. G. In ref 34, p 721.

(36) Puddephatt, R. J. In ref 34, p 772.

(37) Cross, R. J.; Davidson, M. F. *J. Chem. Soc., Dalton Trans.* 1986, 411.

(29) Bruce, M. I.; Horn, E.; Matison, J. G.; Snow, M. R. *J. Organomet. Chem.* 1985, 286, 271.

(30) (a) Sappa, E.; Tiripicchio, A.; Braunstein, P. *Chem. Rev.* 1983, 83, 203. (b) Iggo, J. A.; Mays, M. J.; Raithby, P. R.; Henrick, K. *J. Chem. Soc., Dalton Trans.* 1983, 205. (c) Chetcuti, M. J.; Gordon, J. C.; Green, K. A.; Fanwick, P. E.; Morgenstern, D. *Organometallics* 1989, 8, 1790. (d) Green, M.; Orpen, G.; Schaverien, C. J. *J. Chem. Soc., Dalton Trans.* 1989, 1333. (e) Sappa, E.; Tiripicchio, A.; Manotti-Lanfredi, A. M. *J. Organomet. Chem.* 1983, 249, 391.

(31) Günter, H. *NMR Spectroscopy*; Wiley: New York, 1980; Chapter 2.

(32) Deeming, A. *Adv. Organomet. Chem.* 1986, 26, 1.

(33) Perrin, D. D.; Armarego, W. L. F. *Purification of Laboratory Chemicals*; Pergamon Press: Oxford, U.K., 1988.

**Table 6. Fractional Atomic Coordinates ( $\times 10^4$ ) and Isotropic Thermal Parameters ( $\text{\AA}^2 \times 10^4$ ) with Esd's in Parentheses for the Non-Hydrogen Atoms of Complex 6**

	<i>x/a</i>	<i>y/b</i>	<i>z/c</i>	<i>U</i>
Au	2448(1)	4988(1)	2189(1)	588(1) <sup>a</sup>
Mn(1)	2576(1)	4391(1)	4668(1)	648(6) <sup>a</sup>
Mn(2)	1967(1)	2870(1)	3636(1)	667(5) <sup>a</sup>
Mn(3)	2082(1)	5606(1)	-161(1)	630(5) <sup>a</sup>
Mn(4)	3262(1)	6812(1)	542(2)	744(6) <sup>a</sup>
P(1)	3636(2)	3283(3)	4720(3)	876(13) <sup>a</sup>
P(2)	3036(2)	1809(3)	3580(4)	1047(18) <sup>a</sup>
P(3)	1279(2)	7034(3)	263(3)	792(12) <sup>a</sup>
P(4)	2442(2)	8308(2)	604(3)	848(14) <sup>a</sup>
O(1)	3409(6)	6410(8)	4480(10)	1272(55) <sup>a</sup>
O(2)	2261(6)	3845(9)	7309(7)	1277(46) <sup>a</sup>
O(3)	1201(5)	5906(8)	4690(9)	1197(47) <sup>a</sup>
O(4)	1700(6)	2158(7)	1505(8)	1198(50) <sup>a</sup>
O(5)	1184(6)	937(8)	5321(9)	1368(50) <sup>a</sup>
O(6)	472(5)	4119(8)	3688(10)	1278(49) <sup>a</sup>
O(7)	866(5)	4265(8)	-259(10)	1315(53) <sup>a</sup>
O(8)	2281(7)	6619(10)	-2771(8)	1473(56) <sup>a</sup>
O(9)	3144(5)	3647(8)	-607(8)	1136(43) <sup>a</sup>
O(10)	4202(6)	7697(10)	1840(11)	1561(66) <sup>a</sup>
O(11)	4083(5)	8051(8)	-1773(9)	1289(49) <sup>a</sup>
O(12)	4248(4)	4670(8)	516(9)	1223(43) <sup>a</sup>
O(13)	3706(4)	2210(7)	4081(8)	1049(41) <sup>a</sup>
O(14)	1595(4)	8048(7)	683(8)	1049(41) <sup>a</sup>
O(15)	3765(7)	2619(10)	6056(10)	1614(66) <sup>a</sup>
O(16)	4366(6)	3816(12)	4200(15)	1753(80) <sup>a</sup>
O(17)	2981(7)	496(9)	4358(20)	2464(129) <sup>a</sup>
O(18)	3444(6)	1812(17)	2204(16)	2501(129) <sup>a</sup>
O(19)	912(5)	7908(7)	-767(9)	1175(47) <sup>a</sup>
O(20)	634(4)	6623(7)	1314(9)	1174(45) <sup>a</sup>
O(21)	2342(6)	8964(8)	1623(9)	1264(52) <sup>a</sup>
O(22)	2577(5)	9373(7)	-533(9)	1252(45) <sup>a</sup>
C(1)	3080(6)	5608(10)	4560(10)	802(49) <sup>a</sup>
C(2)	2393(6)	4071(10)	6277(10)	822(54) <sup>a</sup>
C(3)	1719(7)	5319(10)	4618(10)	832(46) <sup>a</sup>
C(4)	1821(6)	2455(8)	2310(11)	840(50) <sup>a</sup>
C(5)	1514(7)	1702(11)	4655(11)	912(54) <sup>a</sup>
C(6)	1058(7)	3703(9)	3677(10)	824(47) <sup>a</sup>
C(7)	1336(6)	4780(10)	-176(11)	898(52) <sup>a</sup>
C(8)	2191(6)	6227(10)	-1712(10)	842(46) <sup>a</sup>
C(9)	2753(7)	4403(11)	-408(10)	867(52) <sup>a</sup>
C(10)	3840(7)	7337(11)	1364(13)	1063(63) <sup>a</sup>
C(11)	3749(7)	7557(10)	-870(13)	998(55) <sup>a</sup>
C(12)	3854(6)	5477(10)	540(11)	894(50) <sup>a</sup>
C(13)	4415(17)	1833(26)	6406(28)	2377(113)
C(14)	4280(15)	1171(23)	7498(26)	2319(109)
C(15)	4686(15)	4224(20)	3173(22)	1877(88)
C(16)	5467(10)	4684(15)	3011(15)	1436(55)
C(17)	3583(24)	-379(36)	4921(36)	3187(202)
C(18)	3382(23)	-1111(35)	5624(37)	2986(185)
C(19)	4113(13)	1664(19)	1650(21)	1829(77)
C(20)	4142(12)	1061(19)	779(20)	1789(75)
C(21)	478(12)	7520(18)	-1410(19)	1660(69)
C(22)	342(16)	8514(25)	-2536(26)	2446(115)
C(23)	44(11)	7432(16)	1692(17)	1616(63)
C(24)	-397(10)	6796(15)	2906(16)	1486(56)
C(25)	2130(11)	8401(18)	2857(21)	1669(69)
C(26)	1490(12)	9025(18)	3434(19)	1819(75)
C(27)	2069(12)	10555(18)	-687(19)	1721(72)
C(28)	1953(13)	10779(22)	-1855(23)	2055(91)

<sup>a</sup> Equivalent isotropic *U*, defined as one-third of the trace of the orthogonalized  $U_{ij}$  tensor.

appropriate addition of water to the commercial material (Aldrich, neutral activity I). Jacketed columns were used, refrigerated by a closed 2-propanol circuit kept at the desired temperature with a cryostat. All other manipulations were carried out at room temperature. <sup>1</sup>H (300.13 MHz), <sup>31</sup>P (121.45 MHz), and <sup>13</sup>C (75.47 MHz) NMR spectra were measured with a Bruker AC300 spectrometer at room temperature, unless otherwise indicated. <sup>1</sup>H{<sup>31</sup>P} NMR spectra were measured at 400.13 MHz on a Bruker AMX instrument. Chemical shifts ( $\delta$ ) are given in ppm, relative to internal TMS (<sup>1</sup>H, <sup>13</sup>C) or external 85% H<sub>3</sub>PO<sub>4</sub> aqueous solution (<sup>31</sup>P), with positive values for frequencies higher than that of the reference. Coupling constants (*J*) are given in Hz.

**Reaction of 1 with [Cu(C≡CPh)]<sub>n</sub>.** Compound 1 (0.100 g, 0.186 mmol) and [Cu(C≡CPh)]<sub>n</sub> (0.030 g, 0.186 mequiv) were stirred in toluene (10 mL) for 5 h, yielding a yellow suspension. Solvent was removed under vacuum, and the residue was extracted first with petroleum ether (3 × 5 mL) and then with dichloromethane. The last fraction yielded, after filtration, removal of solvent under vacuum, and washing of the residue with cold petroleum ether (3 mL, -20 °C), compound 2 as an orange microcrystalline powder (0.038 g, 35%). Similar workup of the petroleum ether fractions yielded compound 4 as a yellow powder (0.045 g, 37%). Anal. Calcd for C<sub>22</sub>H<sub>26</sub>Mn<sub>2</sub>O<sub>11</sub>P<sub>2</sub> (4): C, 41.4; H, 4.1. Found: C, 41.65; H, 4.1. <sup>1</sup>H NMR (C<sub>6</sub>D<sub>6</sub>):  $\delta$  7.6 (d, 2 H, Ph), 7.1–7.0 (m, 3 H, Ph), 3.8–3.7 (m, 8 H, CH<sub>2</sub>), 0.95, 0.90 (2 × t, *J*<sub>HH</sub> = 7, 12 H, CH<sub>3</sub>), -14.5 (t, *J*<sub>PH</sub> = 26, 1 H,  $\mu$ -H). <sup>13</sup>C{<sup>1</sup>H} NMR (CDCl<sub>3</sub>):  $\delta$  220.1 (m, br, 2 × CO), 219.6 (AA'X system, *J*<sub>PC</sub> + *J*<sub>PC</sub> = 40, 2 × CO), 213.2 (AA'X system, *J*<sub>PC</sub> + *J*<sub>PC</sub> = 53, 2 × CO), 132.4, 128.1 (2 × s, C<sup>2</sup>, C<sup>3</sup> [Ph]), 127.5 (s, C<sup>4</sup> [Ph]), 127.2 (s, C<sup>1</sup> [Ph]), 120.0 (t, *J*<sub>PH</sub> = 20, C≡CPh), 89.3 (s, C≡CPh), 62.5, 61.5 (2 × s, OCH<sub>2</sub>), 15.9 (s, Me).

**Reaction of 1 with [Ag(C≡CPh)]<sub>n</sub>.** Compound 1 (0.100 g, 0.186 mmol) and [Ag(C≡CPh)]<sub>n</sub> (0.039 g, 0.186 mequiv) were stirred in toluene (10 mL) in the dark for 5 h, affording a dark yellow suspension, which was filtered. Workup of the filtered solution as described above yielded compound 4 (0.041 g, 35%) and the yellow-orange cluster 5 (0.049 g, 40%). The crystals used for the X-ray study were grown from a CH<sub>2</sub>Cl<sub>2</sub>/petroleum ether mixture at -20 °C. Anal. Calcd for C<sub>28</sub>H<sub>46</sub>Ag<sub>2</sub>Mn<sub>2</sub>O<sub>22</sub>P<sub>4</sub> (5): C, 25.08; H, 3.4. Found: C, 25.3; H, 3.6. <sup>1</sup>H NMR (CD<sub>2</sub>Cl<sub>2</sub>, 250 K):  $\delta$  4.10, 3.97 (2 × m, 2 × 8 H, CH<sub>2</sub>), 1.38, 1.29 (2 × t, *J*<sub>HH</sub> = 7, 2 × 12 H, Me), -7.78 (apparent AA'XX'M system, *J*<sub>HAg</sub> = 105, *J*<sub>HP</sub> + *H*<sub>HP</sub> = 42, 4 H, Ag( $\mu$ -H)Mn), -25.47 (broad t of t, *J*<sub>HP</sub> = 26, *J*<sub>HAg</sub> = 12, 2 H, Mn( $\mu$ -H)Mn). <sup>1</sup>H{<sup>31</sup>P} NMR (CD<sub>2</sub>Cl<sub>2</sub>, 250 K):  $\delta$  -7.82 (pseudodoublet, *J*<sub>HAg</sub> = 105 Hz, Mn( $\mu$ -H)Ag, 4 H), -25.48 (broad t, *J*<sub>HAg</sub> = 12, Mn( $\mu$ -H)Mn, 2 H). <sup>1</sup>H{<sup>31</sup>P} NMR (CD<sub>2</sub>Cl<sub>2</sub>, 290 K):  $\delta$  -7.82 (apparent AA'XX' system, *J*<sub>HAg</sub> + *J*<sub>H'Ag</sub> = 105, Mn( $\mu$ -H)Ag, 4 H), -25.33 (br, Mn( $\mu$ -H)Mn, 2 H).

**Reaction of 1 with [Au(C≡CPh)]<sub>n</sub>.** Compound 1 (0.100 g, 0.186 mmol) and [Au(C≡CPh)]<sub>n</sub> (0.055 g, 0.186 mequiv) were stirred in toluene (10 mL) in the dark for 2.5 h, affording a dark violet mixture. Solvent was removed under vacuum and the residue extracted with petroleum ether and chromatographed on an alumina column (activity III, -20 °C). Elution with petroleum ether gave a yellow fraction containing compound 4. Elution with dichloromethane/petroleum ether (1:10) gave a violet fraction which yielded, after concentration under vacuum and crystallization at -20 °C for 1 day, 0.050 g (42%) of compound 6 as a violet microcrystalline solid. The crystals used in the X-ray diffraction study were grown from a toluene/petroleum ether mixture at -20 °C. Anal. Calcd for C<sub>28</sub>H<sub>46</sub>AuMn<sub>2</sub>O<sub>22</sub>P<sub>4</sub> (6): C, 26.40; H, 3.3. Found: C, 26.65; H, 3.4. <sup>1</sup>H NMR (C<sub>6</sub>D<sub>6</sub>):  $\delta$  3.95, 3.85 (2 × m, 2 × 8 H, CH<sub>2</sub>), 1.12, 1.02 (2 × t, *J*<sub>HH</sub> = 7, 2 × 12 H, Me), -7.63 (quintet, *J*<sub>PH</sub> = 10, 3 H, Au( $\mu$ -H)Mn), -19.34 (t, *J*<sub>PH</sub> = 29, 2 H, Mn( $\mu$ -H)Mn).

**Synthesis of [Mn<sub>2</sub>( $\mu$ -AuP(*p*-tol))<sub>3</sub>( $\mu$ - $\eta^1$ : $\eta^2$ -CH=CHPh)(CO)<sub>6</sub>( $\mu$ -tedip)] (7).** Compound 1 (0.050 g, 0.093 mmol) and [Au(C≡CPh)P(*p*-tol)]<sub>3</sub> (0.056 g, 0.093 mmol) were stirred in toluene (10 mL) for 2 h. The resulting red solution was filtered and concentrated under vacuum to ca. 2 mL. Petroleum ether (3 mL) was then added, and the mixture was stored at -20 °C for 1 day, yielding compound 7 as red crystals (0.07 g, 66%). Anal. Calcd for C<sub>43</sub>H<sub>48</sub>AuMn<sub>2</sub>O<sub>11</sub>P<sub>3</sub>: C, 45.28; H, 4.24. Found: C, 45.57; H, 4.4. <sup>1</sup>H NMR (C<sub>6</sub>D<sub>6</sub>):  $\delta$  7.80 (m, 2 H, Ph), 7.47 (dd, *J*<sub>HH</sub> = 7, *J*<sub>PH</sub> = 12, 6 H, *p*-tol), 7.28 (s, CH=CHPh), 7.13–7.06 (m, 3 H, Ph) 6.80 (d, *J*<sub>HH</sub> = 7, 6 H, *p*-tol), 6.28 (s, 1 H, CH=CHPh), 4.36–4.20 (m, 8 H, OCH<sub>2</sub>), 1.93 (s, 9 H, CCH<sub>3</sub>), 1.42, 1.24, 1.22, 1.19 (4 × t, *J*<sub>HH</sub> = 7, 4 × 3 H, CH<sub>3</sub>). <sup>13</sup>C{<sup>1</sup>H} NMR (CD<sub>2</sub>Cl<sub>2</sub>):  $\delta$  229.0–222.0 (MnCO), 142.3 (s, C<sup>4</sup> [*p*-tol]), 137.4 (s, C<sup>1</sup> [Ph]), 134.3 (d, *J*<sub>PC</sub> = 15, C<sup>2</sup> [*p*-tol]), 132.3 (dd, *J*<sub>PC</sub> = 38, 18, CH=CHPh), 130.2 (d, *J*<sub>PC</sub> = 12, C<sup>3</sup> [*p*-tol]), 128.7, 127.5 (2 × s, C<sup>2</sup> and C<sup>3</sup> [Ph]), 127.8 (s, C<sup>4</sup> [Ph]), 127.7 (d, *J*<sub>PC</sub> = 56, C<sup>1</sup> [*p*-tol]), 121.5 (d, *J*<sub>PC</sub> = 7, CH=CHPh), 62.4–61.9 (OCH<sub>2</sub>), 21.6 (s, CH<sub>3</sub> [*p*-tol]), 16.7–16.1 (CH<sub>2</sub>CH<sub>3</sub>).

**Synthesis of  $[\text{Mn}_2(\mu\text{-AuPPh}_3)(\mu\text{-}\eta^1\text{-}\eta^2\text{-CH=CH}^t\text{Bu})(\text{CO})_6(\mu\text{-thdip})]$  (8).** Compound 1 (0.050 g, 0.093 mmol) and  $[\text{Au}(\text{C}\equiv\text{C}^t\text{Bu})(\text{PPh}_3)]$  (0.030 g, 0.093 mmol) were stirred in toluene (10 mL) for 2 h, affording a red solution. Solvent was then removed under vacuum, and the residue was extracted with petroleum ether. The extractions were chromatographed on an alumina column (activity III, 12 °C). Elution with dichloromethane/petroleum ether (2:3) gave a red fraction which was concentrated under vacuum to ca. 2 mL. Crystallization at -20 °C yielded compound 8 as red crystals (0.007 g, 70%). Anal. Calcd for  $\text{C}_{32}\text{H}_{46}\text{AuMn}_2\text{O}_{11}\text{P}_3$ : C, 42.3; H, 4.3. Found: C, 42.65; H, 4.3.  $^1\text{H NMR}$  ( $\text{CDCl}_3$ ):  $\delta$  7.56–7.46 (m, 5 H, Ph), 6.72 (s, 1 H,  $\text{CH}=\text{CH}^t\text{Bu}$ ), 5.70 (s, 1 H,  $\text{CH}=\text{CH}^t\text{Bu}$ ), 4.23–4.00 (m, 8 H,  $\text{CH}_2$ ), 1.42–1.24 (complex, 12 H,  $\text{CH}_2\text{CH}_3$ ), 1.28 (s, 9 H,  $\text{CCH}_3$ ).  $^{13}\text{C}\{^1\text{H}\}$  NMR ( $\text{CDCl}_3$ ):  $\delta$  134.0 (d,  $J_{\text{PC}} = 14$ ,  $\text{C}^2$  [Ph]), 132.3 (dd,  $J_{\text{PC}} = 40$ , 17,  $\text{CH}=\text{CH}^t\text{Bu}$ ), 131.2 (s,  $\text{C}^4$  [Ph]), 130.8 (d,  $J_{\text{PC}} = 55$ ,  $\text{C}^1$  [Ph]), 129.0 (d,  $J_{\text{PC}} = 11$ ,  $\text{C}^3$  [Ph]), 121.2 (d,  $J_{\text{PC}} = 7$ ,  $\text{CH}=\text{CH}^t\text{Bu}$ ), 61.9–61.3 ( $\text{OCH}_2$ ), 32.95 (s,  $\text{CCH}_3$ ), 32.90 (s,  $\text{CCH}_3$ ), 16.3–15.9 ( $\text{CH}_2\text{CH}_3$ ).

**X-ray Data Collection, Structure Determination, and Refinement for Compounds 5 and 6.** The crystallographic data for both compounds are summarized in Table 4. Data were collected at room temperature (22 °C) on a Siemens AED diffractometer, using niobium-filtered  $\text{Mo K}\alpha$  radiation and the  $\theta/2\theta$  scan type. The reflections for both 5 and 6 were collected with a variable scan speed of 3–12°  $\text{min}^{-1}$  and a scan width from  $(\theta - 0.60)^\circ$  to  $(\theta + 0.60 + 0.346 \tan \theta)^\circ$ . One standard reflection was monitored every 50 measurements; no significant decay was noticed over the time of data collection. The individual profiles have been analyzed by following the method of Lehmann and Larsen.<sup>38</sup> Intensities were corrected for Lorentz and polarization effects. A correction for absorption was applied (maximum and minimum values for the transmission factors were 1.398 and 0.758 for 5 and 1.175 and 0.866 for 6).<sup>39</sup> Only the observed reflections were used in the structure solutions and refinements.

Both structures were solved by Patterson and Fourier methods and refined by full-matrix least squares, first with isotropic thermal parameters and then with anisotropic thermal parameters for the non-hydrogen atoms, with the exception of the carbons of the ethyl groups. With regard to the hydrides, even if in an X-ray structure, determined at room temperature and in the presence of heavy atoms, their accurate location often fails, peaks in plausible positions were found in the final  $\Delta F$  maps. The

positional parameters for three (5) and five (6) hydrides were refined with isotropic thermal parameters. The positions of the hydrides were calculated also by minimization of the potential energy of the intramolecular nonbonded interactions involving the hydrides by using the HYDEX program,<sup>40</sup> and they were comparable with those found in the final  $\Delta F$  map. Because of the remarkable agitation of the ethyl groups, no attempts were made to introduce the hydrogen atoms of these groups in calculated positions. The final cycles of refinement were carried out on the basis of 243 (5) and 472 (6) variables; after the last cycles, no parameters shifted by more than 1.17 (5) and 0.88 (6) esd. The highest remaining peak in the final difference map was equivalent to about 0.29 (5) and 0.33  $\text{e}/\text{Å}^3$  (11). In the final cycles of refinement the weighting scheme  $w = K[\sigma^2(F_o) + gF_o^2]^{-1}$  was used; at convergence the  $K$  and  $g$  values were 0.690 and 0.0063 (5) and 0.633 and 0.0035 (6), respectively. The analytical scattering factors, corrected for the real and imaginary parts of anomalous dispersions, were taken from ref 41. All calculations were carried out on the Cray X-MP/12 computer of the "Centro di Calcolo Elettronico Interuniversitario dell'Italia Nord-Orientale" (CINECA, Casalecchio Bologna) and on the Gould Pownode 6040 of the "Centro di Studio per la Strutturistica Diffattometrica" del CNR, Parma, Italy, using the SHELX-76 and SHELXS-86 systems of crystallographic computer programs.<sup>42</sup> The final atomic coordinates for the non-hydrogen atoms are given in Table 5 (5) and Table 6 (6). The atomic coordinates of the hydrogen atoms are given in Tables SI (5) and SII (6) and the thermal parameters in Tables SIII (5) and SIV (6).

**Acknowledgments.** We thank the Ministerio de Educación y Ciencia of Spain for a grant (to R.C.), the DGICYT of Spain (Project PB91/0678), and Italian Ministero dell'Università e della Ricerca Scientifica e Tecnologica for financial support.

**Supplementary Material Available:** Hydrogen atom coordinates (Tables SI and SII), thermal parameters for the non-hydrogen atoms (Tables SIII and SIV), and all bond distances and angles (Tables SV and SVI) for 5 and 6 (9 pages). Ordering information is given on any current masthead page.

OM930535J

(40) Orpen, A. G. *J. Chem. Soc., Dalton Trans.* 1980, 2509.

(41) *International Tables for X-Ray Crystallography*; Kynoch Press: Birmingham, England, 1974; Vol. IV.

(42) Sheldrick, G. M. SHELX-76 Program for Crystal Structure Determination; University of Cambridge: Cambridge, England, 1976. Sheldrick, G. M. SHELXS-86 Program for the Solution of Crystal Structures; University of Göttingen, Göttingen, Germany, 1986.

(38) Lehmann, M. S.; Larsen, F. K. *Acta Crystallogr., Sect. A* 1974, 30, 580.

(39) Walker, N.; Stuart, D. *Acta Crystallogr., Sect. A* 1983, 39, 158. Ugozzoli, F. *Comput. Chem.* 1987, 11, 109.